DOI: 10.1002/asia.200700242

Oligomeric Alkoxysilanes with Cagelike Hybrids as Cores: Designed Precursors of Nanohybrid Materials

Hideki Kuge,[a] Yoshiaki Hagiwara,[a] Atsushi Shimojima,*[c, d] and Kazuyuki Kuroda *[a, b, c]

Abstract: Well-defined alkoxysilane oligomers containing a cagelike carbosiloxane core were synthesized and used as novel building blocks for the formation of siloxane-based hybrid networks. These oligomers were synthesized from the cagelike trimer derived from bis(triethoxysilyl)methane by silylation with mono-, di-, and triethoxychlorosilanes ($(EtO)_nMe_{3-n}SiCl$, $n=1$, 2, and 3). Hybrid xerogels were prepared by hydrolysis and polycondensation of these oligomers under acidic conditions. The structures of the products varied depending on the number of alkoxy groups (n). When $n=2$ and 3, microporous xerogels (BET surface areas of 820 and 510 m^2g^{-1}, respectively) were obtained, whereas a nonporous xerogel was obtained when $n=1$. ^{29}Si NMR spectroscopic analysis suggested that partial rearrangement of the siloxane networks, which accompanied the cleavage of the Si–O–Si linkages, occurred during the polycondensation processes. By using an amphiphilic triblock copolymer surfactant as a structure-directing agent, hybrid thin films with a 2D hexagonal mesostructure were obtained when $n=2$ and 3. These results provide important insight into the rational synthesis of molecularly designed hybrid materials by sol–gel chemistry.

Keywords: mesoporous materials · organic–inorganic hybrid composites · self-assembly · siloxanes · sol–gel processes

Introduction

Siloxane–organic hybrid materials prepared by sol–gel chemistry have received both fundamental and practical interest.[1] Significant progress has been made in tailoring the structure and properties of the products by the molecular design of alkoxysilane precursors.[2,3] Furthermore, in recent years, the surfactant-directed self-assembly process has been developed as a tool for producing various hybrid mesostructures (lamellar, hexagonal, cubic, etc.).[4,5] However, precise control over local structures and the molecular homogeneity of sol–gel-derived hybrid solids is still difficult. This is an important issue particularly in multicomponent systems with more than two types of monomers because of the difference in the reaction rates caused by inductive and/or steric effects.[6] In this context, a promising approach should be the use of predesigned oligomeric alkoxysilanes as molecular building blocks.

Among the various types of oligomeric species, those with cagelike structures are important because of their rigid and symmetrical frameworks. Silsesquioxane cages ($(RSiO_{1.5})_n$, R = H or organic groups) can be obtained by controlled hydrolysis and polycondensation of trifunctional organosilanes ($RSiCl_3$ or $RSi(OR')_3$).[7,8] It is also known that cagelike olig-

[a] H. Kuge, Y. Hagiwara, Prof. K. Kuroda
Department of Applied Chemistry
Waseda University, Ohkubo-3, Shinjuku-ku
Tokyo, 169-8555 (Japan)
Fax: (+81) 3-5286-3199
E-mail: kuroda@waseda.jp

[b] Prof. K. Kuroda
Kagami Memorial Laboratory for
Materials Science and Technology
Waseda University, Nishiwaseda-2, Shinjuku-ku
Tokyo, 169-0051 (Japan)

[c] Dr. A. Shimojima, Prof. K. Kuroda
Core Research for Evolutional Science and Technology (CREST)
Japan Science and Technology Agency (JST)
Honcho 4-1-8, Kawaguchi-shi
Saitama, 332-0012 (Japan)

[d] Dr. A. Shimojima
Department of Chemical System Engineering
The University of Tokyo, Hongo-7, Bunkyo-ku
Tokyo 113-8656 (Japan)
E-mail: shimoji@chemsys.t.u-tokyo.ac.jp

Supporting information for this article is available on the WWW under http://www.chemasianj.org or from the author.

omers such as $Si_6O_{15}^{6-}$, $Si_8O_{20}^{8-}$, and $Si_{10}O_{25}^{10-}$ are formed in alkaline silicate solutions containing quaternary ammonium cations.[9] Such cagelike species serve not only as "building blocks" for the synthesis of silica-based materials, but also as "cores" for the design of even larger building blocks.[9–15] Silylation of the cage corners is a well-established method for producing larger siloxane species.[9] However, most of the products reported so far have been derivatized with organosilyl (R_3Si) groups, which cannot be employed in the sol–gel process. To overcome this limitation, we recently succeeded in the synthesis of alkoxysilylated derivatives of cubic octameric silicates (double-four-ring silicates) by silylation with a series of alkoxychlorosilanes ($(EtO)_nMe_{3-n}SiCl$, $n=1, 2, 3$).[16]

Organoalkoxysilanes containing organic spacers, $(R'O)_3Si–R–Si(OR')_3$, are widely used to produce unique hybrids in which organic groups are integrated into their frameworks. Extensive studies have been carried out on xerogels[17,18] and mesostructured solids.[19,20] However, such materials are generally formed by random cross-linking of monomers, which involves the formation of linear and cyclic oligomers at the initial stages;[21] therefore, the design of well-defined oligomeric units is of great importance. We reported the synthesis of cagelike trimers by hydrolysis and polycondensation of bis(triethoxysilyl)methane ($(EtO)_3Si–CH_2–Si(OEt)_3$, BTESM) in the presence of tetramethylammonium (TMA) hydroxide.[22] One of the isomers (Scheme 1) was selectively formed under certain conditions. It is analogous to double-three-ring silicates ($Si_6O_{15}^{6-}$), except that the bridging oxygen atoms are partially replaced by methylene groups. The presence of Si–O^- (or Si–OH) sites at the cage corners allows further chemical modifications, thus making it a good candidate as building blocks or scaffolds for the potential synthesis of a new class of hybrid materials.

Abstract in Japanese:
かご型カルボシロキサンをコアとした明確な分子構造をもつ3種のアルコキシシランオリゴマーを合成し、それぞれ新規なビルディングブロックとして用いることでシロキサン系ハイブリッド構造体を得た。これらのオリゴマーはビス（トリエトキシシリル）メタンから得られるかご型3量体を、モノ-、ジ-、トリエトキシクロロシラン [$(EtO)_nMe_{3-n}SiCl$, n = 1, 2, 3] を用いてシリル化することによって合成した。酸性条件下での加水分解・縮重合反応によって、アルコキシ基数の違いによりそれぞれ異なる構造のハイブリッドキセロゲルを得た。n = 2, 3 のとき、ミクロ多孔体のキセロゲル (BET 表面積 820, 510 $m^2 g^{-1}$) を得たが、n = 1 のときは無孔質であった。^{29}Si NMR 分析の結果から、縮重合過程でシロキサン結合の開裂を伴って部分的にネットワークが再配列していることが示された。n = 2, 3 のオリゴマーを用いた場合、両親媒性トリブロックコポリマーを構造制御剤として用いることにより、2次元ヘキサゴナル構造のハイブリッド薄膜を得ることにも成功した。以上の結果は、ゾルゲルプロセスによって分子レベルで設計されたハイブリッド材料を構築するための重要な知見を与えるものである。

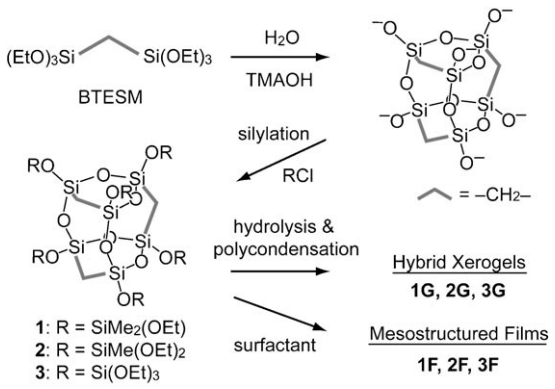

Scheme 1. Design of hybrid materials by using alkoxysilylated derivatives of cagelike oligomers derived from bis(triethoxysilyl)methane (BTESM).

Herein, we report the molecular design of mono-, di-, and trialkoxysilylated derivatives of the cagelike trimer derived from BTESM (**1**, **2**, and **3** in Scheme 1) by silylation with corresponding alkoxychlorosilanes ($(EtO)_nMe_{3-n}SiCl$, $n=1$, 2, 3). To understand the chemistry of these oligomeric species, their hydrolysis and polycondensation behavior under acidic conditions as well as the structure and porosity of the resulting xerogels were studied in detail. Furthermore, mesostructured thin films were prepared by using a poly(oxyethylene)–poly(oxypropylene)–poly(oxyethylene) (PEO–PPO–PEO)-type amphiphilic triblock copolymer ($EO_{20}PO_{70}EO_{20}$) as a structure-directing agent, which represents a promising approach to hierarchically ordered hybrid materials.

Results and Discussion

Characterization of 1, 2, and 3

As we reported previously,[22] the cagelike trimer derived from BTESM consists of two inequivalent Si sites. In its ^{29}Si NMR spectrum, two signals (−56.0 and −59.1 ppm) corresponding to the T^2 units[23] appear with the intensity ratio 1:2. Figure 1A shows the liquid-state ^{29}Si NMR spectra of **1**, **2**, and **3** synthesized by alkoxysilylation of this cagelike trimer. The spectrum of **1** shows mainly four signals (Figure 1A, spectrum a). Two close signals at −11.0 and −11.3 ppm correspond to the D^1 units,[23] and the other two signals at −61.9 and −65.7 ppm correspond to the T^3 units. Oligomers **2** and **3** exhibit T^1 (−50.3 ppm with a shoulder) and Q^1 signals (−88.7, −88.8 ppm),[23] respectively, in addition to the T^3 signals. The absence of T^2 signals in all the spectra suggests the complete silylation of the cagelike trimer, although the appearance of small, unidentified signals indicates the presence of other species. Also, the retention of the ethoxy groups without hydrolysis was confirmed by ^{13}C NMR spectra (data not shown), which showed the signals of Si–OCH_2CH_3 (at around 18 and 59 ppm).

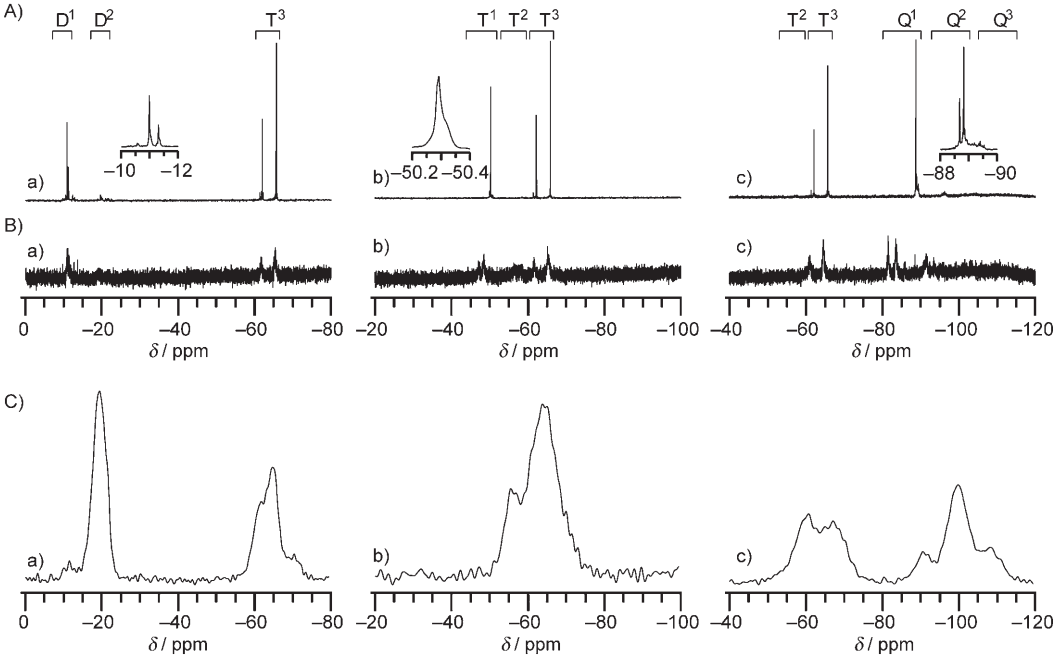

Figure 1. A) Liquid-state ^{29}Si NMR spectra of a) **1**, b) **2**, and c) **3** in $CDCl_3$. B) Liquid-state ^{29}Si NMR spectra of solutions of a) **1**, b) **2**, and c) **3** after 1 h of reaction. C) Solid-state ^{29}Si MAS NMR spectra of the xerogels a) **1G**, b) **2G**, and c) **3G**.

Hydrolysis and Polycondensation Processes

Hydrolysis and polycondensation of **1**, **2**, and **3** were performed under acidic conditions to minimize the decomposition of the oligomers by hydrolysis of Si–O–Si bonds, which occurs much faster under basic conditions.[6] We studied the reaction processes by liquid-state ^{29}Si NMR. To monitor the initial stage of the reactions, the HCl/Si molar ratio was decreased to 1/10 of that employed in the xerogel syntheses. Figure 1B shows the ^{29}Si NMR spectra of the solutions after 1 h of reaction. Several signals indicative of hydrolysis and condensation of terminal Si–OEt groups were observed along with the T^3 signal of the cagelike cores. In the case of **1** (Figure 1B, spectrum a), a small signal slightly upfield of that of the D^1 unit can be assigned to the $D^1_{(1OH)}$ unit, and the signals at around −20 ppm can be assigned to the D^2 units.[24] The spectrum for **2** (Figure 1B, spectrum b) shows broad signals at −48 and −46 ppm, which were assigned to the $T^1_{(1OH)}$ and $T^1_{(2OH)}$ units,[25] respectively, and a broad T^2 signal at around −58 ppm. In Figure 1B, spectrum c, the signals due to the hydrolyzed $Si(OEt)_3$ groups of **3** ($Q^1_{(3OH)}$, $Q^1_{(2OH)}$, and $Q^1_{(1OH)}$ units) were observed at around −82, −84, and −86 ppm, respectively, together with the Q^2 signals.[6] Further reaction led to ill-resolved spectra, which is attributed to the formation of polymerized species (see Supporting Information).

We note here that the intramolecular condensation between adjacent terminal silyl groups is sterically hindered, similar to the case of the alkoxysilylated derivatives of cubic octameric silicate.[16] Therefore, the appearance of the D^2, T^2, and Q^2 signals in the hydrolyzed solutions of **1**, **2**, and **3** (Figure 1B), respectively, suggest that the intermolecular condensation proceeded after hydrolysis of the Si–OEt groups. The considerably broad T^3 signals of the cagelike cores should be attributed to the various environments of the terminal silyl groups bonded to the cores. Notably, the signals due to the D^0, T^0, and Q^0 units did not appear during the reaction. This suggests that the cleavage of the Si–O–Si linkages between the terminal silyl groups and the cores are very slow relative to hydrolysis and polycondensation of the terminal Si–OEt groups. Thus, we confirmed that the original siloxane frameworks of **1**, **2**, and **3** are retained at the initial stage of the reactions.

The slow rate of hydrolysis of Si–O–Si bonds under our experimental conditions was actually confirmed by using the trimethylsilylated derivative,[22] in which inert $Si–CH_3$ groups were substituted for the hydrolyzable Si–OEt groups of **1**–**3**. When this molecule was treated for 1 day under conditions similar to those for the synthesis of **3G**,[26] new signals due to the T^2 (at around −53 and −57 ppm), M^0 (13.2 ppm), and M^1 (7.3 ppm) units appeared in the ^{29}Si NMR spectrum (see Supporting Information). The M^0 and M^1 signals can be assigned to Me_3SiOH and $Me_3Si–O–SiMe_3$, respectively,[27] which suggests that the cleavage of the Si–O–Si bonds linking the core and the terminal trimethylsilyl groups proceeded. However, the degree of cleavage was only about 20% as estimated from the relative-intensity ratios.

Hydrolysis and polycondensation of **1**, **2**, and **3** led to gelation within 1 day. This behavior is different from that observed for mixtures of monomeric alkoxysilanes (i.e., dimethyldiethoxysilane (DMDES)–, methyltriethoxysilane (MTES)–, and tetraethoxysilane (TEOS)–BTESM mixtures),[28] which did not form gels even after 1 day of reaction. The faster gelation of the oligomeric precursors should

be due to their larger molecular size, which allows efficient growth of the siloxane networks. Although transparent gels were obtained from **2** and **3**, an opaque gel was formed from **1**. This may be due to the microphase separation between rather hydrophobic polymers formed from dimethylsilyl-terminated oligomers and the water-based hydrophilic phase. In fact, the scanning electron microscopy (SEM) image of **1G** (data not shown) revealed the presence of large spherical voids possibly formed by phase separation.

Characterization of the Xerogels

The xerogels **1G**, **2G**, and **3G** were characterized by solid-state ^{29}Si magic-angle spinning (MAS) NMR to obtain information on the siloxane networks. The spectrum of **1G** (Figure 1C, spectrum a) shows mainly a D^2 signal (−19 ppm) and two T^3 signals (−61 and −64 ppm). The signal due to the $SiMe_2(OEt)$ groups (D^1 unit, at −12 ppm) is very small, which suggests that almost all the silyl groups at the cage corners are linked together by siloxane bonds. The appearance of another T^3 signal at 70 ppm is probably due to the partial rearrangement of the siloxane networks. In the case of **2G**, only T^2 and T^3 signals (−56 and −64 ppm, respectively) were observed (Figure 1C, spectrum b). The absence of a T^1 signal confirmed that all the terminal $SiMe(OEt)_2$ groups of **2** were hydrolyzed and polycondensed to form at least one siloxane bond. However, more detailed analysis of this spectrum could not be performed because of the overlapping of the signals of the cagelike cores and the terminal silyl groups. The spectrum of **3G** shows Q^2, Q^3, and Q^4 signals (−92, −100, and −108 ppm, respectively) along with the T^2 and T^3 signals (Figure 1C, spectrum c). The presence of the T^2 units clearly confirms that the Si–O–Si linkages were partially cleaved during polycondensation. However, deconvolution of the signals to estimate the degree of cleavage was unsuccessful because the T^3 signal of the core appears close to the T^2 region (−55 to −60 ppm).

The difference in the number of alkoxy groups, that is, the difference in the degree of cross-linking between the cagelike cores, resulted in different properties for the xerogels. The thermogravimetry differential thermal analysis (TG-DTA) curves for **2G** and **3G** display endothermic peaks accompanied by an approximately 15% mass loss below 100 °C (Figure 2), which can be due to the loss of adsorbed water molecules. In contrast, no such peak was observed for **1G**, which suggests that the xerogel has a relatively hydrophobic network. In fact, in the IR spectra of these xerogels (see Supporting Information), strong bands due to H_2O (at 3100–3600 and 1600 cm^{-1}) were observed for **2G** and **3G**, whereas **1G** exhibited much weaker bands in these regions. At higher temperature, large exothermic peaks with weight losses indicative of combustion of organic moieties (methyl and/or methylene groups) were observed at about 420, 560, and 600 °C for **1G**, **2G**, and **3G**, respectively. The gradual mass losses starting from 200 °C observed for both **2G** and **3G** suggest that a part of the organic moieties were combusted. Interestingly, the thermal stabilities of **2G** and **3G**

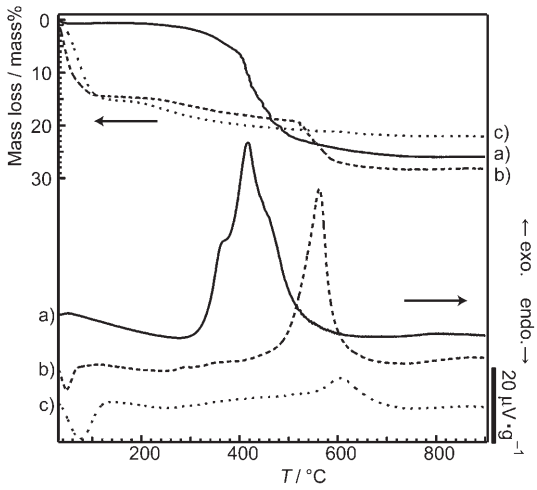

Figure 2. TG-DTA curves for the xerogels a) **1G**, b) **2G**, and c) **3G**. endo. = endothermic, exo. = exothermic.

are higher than those of the xerogels derived from the MTES–BTESM and TEOS–BTESM mixtures,[28] which showed exothermic peaks at about 510 and 550 °C, respectively (see Supporting Information). This should be due to the difference in the local structure of the hybrid xerogels, although the detailed behavior is still under investigation.

The number of alkoxy groups in the oligomers also affected the porosity of the resulting xerogels. Figure 3 shows the nitrogen-adsorption isotherms of **1G**, **2G**, and **3G**. The isotherms of **2G** and **3G** display the type I curve, which suggests that they are microporous. The Brunauer–Emmett–Teller (BET) surface areas of **2G** and **3G** were calculated to be 820 and 510 $m^2 g^{-1}$, respectively. These samples have an average pore diameter of 0.6 nm, which can be calculated either by the Saito–Foley (SF) method or by the Barrett–Joyner–Halenda (BJH) method. In contrast, **1G** exhibits a very low BET surface area (< 10 $m^2 g^{-1}$). Despite this difference in porosity, no difference in the microstructures was

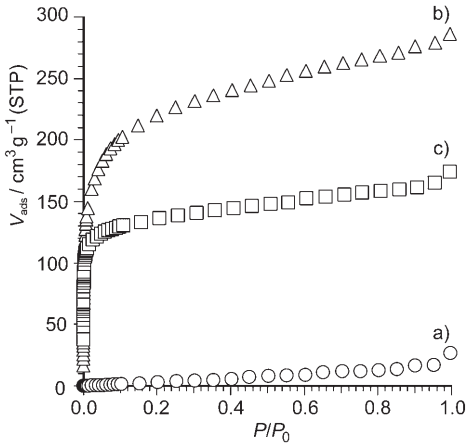

Figure 3. Nitrogen-adsorption isotherms of a) **1G**, b) **2G**, and c) **3G**.

observed by TEM (see Supporting Information for the images of **1G** and **3G**).

The nonporous nature of **1G** is probably due to its relatively flexible networks, which form only one siloxane bond at each corner of the cagelike unit, thus causing large shrinkage of the networks during the drying process. Interestingly, highly porous xerogels were obtained from **3**, which is in contrast to our previous finding that a triethoxysilylated derivative of cubic octameric silicate had a very low BET surface area. This difference is possibly associated with the deterioration of **3** during hydrolysis and polycondensation, as evidenced by ^{29}Si MAS NMR.

Preparation of Mesostructured Films

Mesoscale self-assembly of oligomers **1**, **2**, and **3** by using a surfactant as the structure-directing agent was performed to construct hybrid materials with structural hierarchy. Although various mesostructured hybrids have been synthesized starting from monomeric alkoxysilanes including BTESM,[29,30] there have been only a few reports on the use of well-defined oligomeric species.[16,31,32] We used amphiphilic triblock copolymer P123 because it appeared to be large enough to direct the self-assembly of the oligomeric species consisting of 12 Si atoms.

Figure 4 shows the XRD patterns of the thin films (**1F**, **2F**, and **3F**) prepared by hydrolysis and polycondensation of **1**, **2**, and **3** in the presence of P123. Although **1F** is non-ordered, **2F** and **3F** exhibit sharp diffraction peaks ($d = 9.40$ and 9.17 nm, respectively) accompanied by second-order reflections. The periodic structures were retained even after calcination ($d = 5.60$ and 6.77 nm), and the TEM images of **3F** after calcination (Figure 5) display either honeycomb or striped patterns, thus confirming the 2D hexagonal mesostructure of the film. The two XRD peaks were therefore indexed as the (10) and (20) reflections of the 2D hexagonal structure. The absence of a (11) peak suggests that the mesochannels are oriented parallel to the substrate surface.[33]

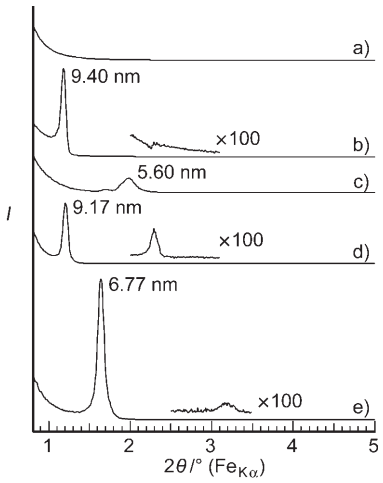

Figure 4. XRD patterns of a) **1F**, b) **2F**, c) calcined **2F**, d) **3F**, and e) calcined **3F**.

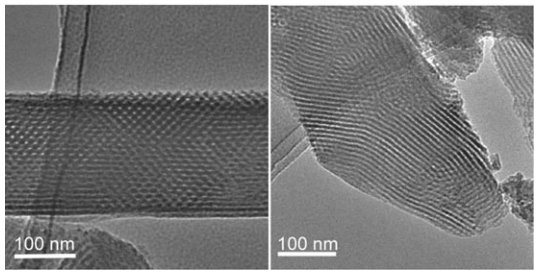

Figure 5. Typical TEM images of calcined **3F** showing the honeycomb (left) and striped (right) patterns.

The TEM images of the calcined **2F** also showed the presence of mesopores (see Supporting Information). However, the structure is less ordered relative to **3F**, which should be due to the thermally less stable network of **2F**, as expected from the significant decrease in the intensity of the XRD peak upon calcination.

FTIR analysis suggests that surfactants in the films were mostly removed by calcination while maintaining the Si–CH_2–Si linkage. Figure 6a and b show the IR spectra of **3F** before and after calcination, respectively. The spectrum of **3G** (Figure 6c) is also shown for comparison. Before calcination, four absorption peaks due to C–H stretching modes were observed in the range 2850–3000 cm^{-1}. The peaks at 2900 and 2970 cm^{-1} were assigned to the CH_3 groups of P123, and the other peaks at about 2850 and 2925 cm^{-1} were assigned to the CH_2 groups of both P123 and the cagelike cores. After calcination, the CH_3 peaks significantly decreased and became smaller than the CH_2 peaks, which suggests that most of the surfactant was removed. We also note that the band at about 700 cm^{-1}, which is likely to be associated with the Si–CH_2–Si linkages, was still observed after calcination (data not shown). The removal of the surfactant by calcination was supported by the nitrogen-adsorption measurements. The isotherm for **3F** after calcination shows a type IV curve typical of mesoporous silica (see Supporting Information).

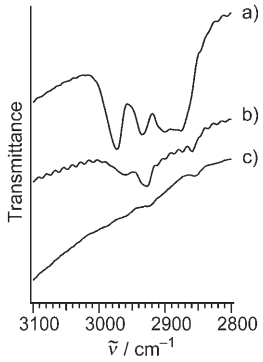

Figure 6. FTIR spectra (C–H stretching region) of a) **3F**, b) calcined **3F**, and c) **3G**.

It is generally recognized that the interactions (mainly hydrogen-bonding) between siloxane species and PEO blocks are essential for the formation of hybrid mesostructures when PEO-based surfactants are used.[34] In the present systems, the lack of structural order in **1F** should be due to a relatively weak interaction of hydrolyzed **1** with PEO blocks of the surfactant (P123). This is reasonable because of the smaller number of Si–OH groups and the relatively hydrophobic nature of **1**, which has 12 terminal methyl groups. A

similar result was obtained in our recent study with a monoethoxysilylated derivative of cubic octameric silicate as precursors.[16] It is therefore concluded that geminal silanol groups ($Si(OH)_2$) at the cage corners are necessary for the building blocks to interact fully with PEO blocks to form mesostructures.

Mesoporous hybrid films are potentially useful as low-k dielectrics and low-refractive-index materials.[35] Besides the mesoporosity generated by surfactant templates, it is important to control the compositions and local structure of the hybrid networks. The incorporation of methyl and methylene groups in the networks contributes to an increase in hydrophobicity and a decrease in dielectric constant relative to pure silica mesoporous films.[36–38] The use of well-defined building blocks may lead to fine-tuning of the physical properties of the hybrid films, and further characterization of these films in this regard is underway.

Conclusions

We have demonstrated the formation of siloxane-based hybrid materials by using three new types of molecular building blocks in which mono-, di-, and trialkoxysilyl groups are attached to the cagelike hybrid core. Detailed analysis of the hydrolysis and polycondensation processes of these oligomers suggested that novel hybrid xerogels containing cagelike units have been prepared, although partial cleavage of Si–O–Si linkages occurred during the synthesis. The tuning of the structure and properties of the xerogels was accomplished by varying the number of alkoxy groups. Furthermore, we have succeeded in the synthesis of mesostructured hybrid films by using a triblock copolymer surfactant as a structure-directing agent. These results provide important insight into the precise design of hybrid materials at scales of various orders of magnitude.

Experimental Section

*Synthesis of Precursors (**1**, **2**, and **3**)*

The synthesis of the cagelike trimers from BTESM was performed according to our previous report.[22] Starting from a mixture with a BTESM/ethanol/H_2O/TMAOH molar ratio of 1:20:20:3, the cagelike trimer shown in Scheme 1 was formed almost quantitatively. Mono-, di-, and triethoxychlorosilanes ($(EtO)Me_2SiCl$, $(EtO)_2MeSiCl$, and $(EtO)_3SiCl$) containing $Me_2Si(OEt)_2$ ($\approx$10%), $MeSi(OEt)_3$ ($\approx$30%), and $Si(OEt)_4$ ($\approx$50%), respectively,[16] were used as the silylating agents. Typically, 5 mL of the mixture containing the cagelike trimers was added to a mixture of an excess of the silylating agent (0.61 mol), THF (100–150 mL), and pyridine (32 mL). After stirring for 30 min, volatile components were removed in vacuo to yield white solids containing the silylated derivatives, TMACl, and pyridine hydrochloride. Extraction with hexane (50 mL) followed by removal of the solvent in vacuo afforded a viscous liquid. The alkoxysilylated derivatives (**1**, **2**, and **3**) were finally isolated by gel-permeation chromatography (GPC) as clear, colorless liquids (yields: $\approx$45% based on BTESM).

1: ^{1}H NMR (500 MHz, $CDCl_3$): 0.04, 0.11, 0.14, 0.24, 0.27, 1.21, 3.76 ppm (some signals may have overlapped with the large signal of methyl protons); ^{13}C NMR (125.7 MHz, $CDCl_3$): $\delta = -1.2$, -1.0, 0.2, 0.7, 1.0, 18.4, 58.0 ppm; ^{29}Si NMR (99.3 MHz, $CDCl_3$): -11.0, -11.3, -61.9, -65.7 ppm; MS (FAB): m/z calcd for $C_{27}H_{72}O_{18}Si_{12}$: 1020.1 $[M+H]^+$; found: 1021.0.

2: ^{1}H NMR (500 MHz, $CDCl_3$): $\delta = -0.14$, -0.01, 0.11, 0.16, 0.19, 1.07, 3.67 ppm (some signals may have overlapped with the large signal of methyl protons); ^{13}C NMR (125.7 MHz, $CDCl_3$): $\delta = -5.6$, -0.9, 18.2, 58.3 ppm; ^{29}Si NMR (99.3 MHz, $CDCl_3$): -50.3, -50.3, -62.2, -65.7 ppm; MS (FAB): m/z calcd for $C_{33}H_{84}O_{24}Si_{12}$: 1200.2 $[M+H]^+$; found: 1201.2.

3: ^{1}H NMR (500 MHz, $CDCl_3$): $\delta = -0.25$, 0.21, 0.23, 1.24, 3.84 ppm; ^{13}C NMR (125.7 MHz, $CDCl_3$): $\delta = -1.0$, -0.2, 18.1, 59.3 ppm; ^{29}Si NMR (99.3 MHz, $CDCl_3$): $\delta = -61.9$, -65.7, -88.7, -88.8 ppm; MS (FAB): m/z calcd for $C_{39}H_{96}O_{30}Si_{12}$: 1380.3 $[M+H]^+$; found: 1381.2.

Synthesis of Hybrid Xerogels

Hybrid xerogels **1G**, **2G**, and **3G** were prepared by hydrolysis and polycondensation of **1**, **2**, and **3**, respectively, in mixtures of THF, H_2O, and HCl. The molar ratios were **1**/ethanol/H_2O/HCl = 1:36:6:0.06, **2**/ethanol/H_2O/HCl = 1:36:12:0.06, and **3**/ethanol/H_2O/HCl = 1:36:18:0.06; the H_2O/OEt ratios were adjusted to 1. The mixtures were stirred at room temperature for 1 h and then allowed to stand for 1 day, during which gelation occurred in the closed vessels. The solvents were evaporated under reduced pressure to produce xerogels, which were pulverized before characterization.

Synthesis of Mesostructured Hybrid Films

Mesostructured thin films **1F**, **2F**, and **3F** were prepared from **1**, **2**, and **3**, respectively, by reaction in the presence of amphiphilic triblock copolymer surfactant $EO_{20}PO_{70}EO_{20}$ (Sigma–Aldrich). The oligomers were prehydrolyzed by stirring in a mixture of ethanol, H_2O, and HCl at room temperature for 2 h, and then a solution of P123 in ethanol was added. The final molar ratio of the mixture was **1** (or **2** or **3**)/ethanol/H_2O/HCl/P123 = 1.0:456:99.6:0.50:0.12. These precursor solutions were spin-coated on glass substrates and air-dried at room temperature for 2 days. The films **2F** and **3F** were further calcined in air at 593 K for 4 h (heating rate 2 K min^{-1}) to remove the surfactant.

Characterization

Liquid-state ^{29}Si NMR spectra were obtained on a JEOL Lambda-500 spectrometer with resonance frequencies of 99.25 MHz. The sample solutions were put in 5-mm glass tubes, tetramethylsilane (TMS) was added as an internal reference, and $CDCl_3$ or $[D_6]$ethanol was used to obtain lock signals. A small amount of $Cr(acac)_3$ (acac = acetylacetonate) was also added as a relaxation agent for ^{29}Si nuclei. XRD patterns were recorded on a Mac Science M03XHF22 diffractometer with Mn-filtered $Fe_{K\alpha}$ radiation. TEM images were obtained on a JEOL JEM-2010 microscope operating at 200 kV. To prepare the TEM samples, the xerogels or mesostructured films scraped off from the substrate were ground with a mortar and pestle and dispersed in ethanol. A carbon-coated TEM grid was dipped in the dispersion and, after withdrawal, was dried in air. Solid-state ^{29}Si MAS NMR spectroscopy was performed on a JEOL JNM-CMX-400 spectrometer at a resonance frequency of 79.42 MHz, with a pulse width of 45° and a recycle delay of 100 s. Positive FAB mass spectra were obtained by using a JEOL JMS-SX-102A mass spectrometer. FTIR spectra of the products in KBr pellets were obtained on a Perkin–Elmer Spectrum One spectrometer with a nominal resolution of 0.5 cm^{-1}. Nitrogen-adsorption measurements were performed by an Autosorb-1 instrument (Quantachrome Instruments, Inc.) at 77 K. Samples were preheated at 120 °C for 3 h under about 1.3 Pa pressure. TG-DTA was carried out with a RIGAKU TG8120 instrument under a dry air flow at a heating rate of 10 K min^{-1}.

Acknowledgements

We are grateful to Dr. Dai Mochizuki, Ms. Mikako Sakurai, Mr. Yoshiyuki Kuroda, Mr. Ryota Goto, Mr. Ryutaro Wakabayashi, and Mr. Kazufu-

mi Kawahara (Waseda University) for experimental help. This work was supported in part by a Grant-in-Aid for Scientific Research (No. 18350110), the 21st Century COE Program "Practical Nano-Chemistry", and the Global COE program "Practical Chemical Wisdom" from MEXT, Japan. The A3 Foresight Program "Synthesis and Structural Resolution of Novel Mesoporous Materials" supported by the Japan Society for the Promotion of Science (JSPS) is also acknowledged.

[1] *Special Issue on Functional Hybrid Materials* (Ed.: C. Sanchez), *J. Mater. Chem.* **2005**, *15* (35–36).
[2] C. Sanchez, F. Ribot, *New J. Chem.* **1994**, *18*, 1007–1047.
[3] R. J. P. Corriu, D. Leclercq, *Angew. Chem.* **1996**, *108*, 1524–1540; *Angew. Chem. Int. Ed. Engl.* **1996**, *35*, 1420–1436.
[4] L. Nicole, C. Boissiére, D. Grosso, A. Quach, C. Sanchez, *J. Mater. Chem.* **2005**, *15*, 3598–3627.
[5] F. Hoffmann, M. Cornelius, J. Morell, M. Fröba, *Angew. Chem.* **2006**, *118*, 3290–3328; *Angew. Chem. Int. Ed.* **2006**, *45*, 3216–3251.
[6] C. J. Brinker, G. W. Scherer, *Sol–Gel Science: The Physics and Chemistry of Sol–Gel Processing*, Academic Press, San Diego, **1990**.
[7] P. A. Agaskar, *Inorg. Chem.* **1991**, *30*, 2707–2708.
[8] A. R. Bassindale, Z. Liu, I. A. MacKinnon, P. G. Taylor, Y. Yang, M. E. Light, P. N. Horton, M. B. Hursthouse, *Dalton Trans.* **2003**, 2945–2949.
[9] P. G. Harrison, *J. Organomet. Chem.* **1997**, *542*, 141–183, and references therein.
[10] V. W. Day, W. G. Klemperer, V. V. Mainz, D. M. Millar, *J. Am. Chem. Soc.* **1985**, *107*, 8262–8264.
[11] C. A. Fyfe, G. Fu, *J. Am. Chem. Soc.* **1995**, *117*, 9709–9714.
[12] G. H. Mehl, I. M. Saez, *Appl. Organomet. Chem.* **1999**, *13*, 261–272.
[13] D. Hoebbel, K. Endres, T. Reinet, I. Pitsch, *J. Non-Cryst. Solids* **1994**, *176*, 179–188.
[14] R. M. Laine, *J. Mater. Chem.* **2005**, *15*, 3725–3744.
[15] R. E. Morris, *J. Mater. Chem.* **2005**, *15*, 931–938.
[16] Y. Hagiwara, A. Shimojima, K. Kuroda, *Chem. Mater.*, DOI: 10.1021/cm0716194
[17] K. J. Shea, D. A. Loy, *Chem. Mater.* **2001**, *13*, 3306–3319.
[18] R. J. P. Corriu, J. J. E. Moreau, P. Thepot, M. C. M. Wong, *Chem. Mater.* **1992**, *4*, 1217–1224.
[19] S. Inagaki, S. Guan, Y. Fukushima, T. Ohsuna, O. Terasaki, *J. Am. Chem. Soc.* **1999**, *121*, 9611–9614.
[20] T. Asefa, C. Yoshina-Ishii, M. J. MacLachlan, G. A. Ozin, *J. Mater. Chem.* **2000**, *10*, 1751–1755.
[21] K. J. Shea, D. A. Loy, *Acc. Chem. Res.* **2001**, *34*, 707–716.
[22] A. Shimojima, K. Kuroda, *Chem. Commun.* **2004**, 2672–2673.
[23] The chemical shifts of Si atoms are largely influenced by the number of Si–C bonds and siloxane (Si–O–Si) bonds. The symbols D^n, T^n, and Q^n represent $C_2Si(OSi)_n(OX)_{2-n}$, $CSi(OSi)_n(OX)_{3-n}$, and $Si(OSi)_n(OX)_{4-n}$, in which X = R or H. The number of OH groups are also depicted as subscripts.
[24] Y. Sugahara, S. Okada, K. Kuroda, C. Kato, *J. Non-Cryst. Solids* **1992**, *139*, 25–34.
[25] Y. Sugahara, S. Okada, K. Kuroda, C. Kato, *J. Non-Cryst. Solids* **1994**, *167*, 21–28.
[26] Because of the low solubility of the crystalline trimethylsilylated derivative in the mixture of ethanol and H_2O, THF (the volume ratio of THF/ethanol was 1:1) was added to obtain a homogeneous solution. The final molar ratios were trimethylsilylated derivative/ethanol (containing 10 vol% of [D_6]ethanol)/THF/H_2O/HCl = 1:36:26:18:0.06.
[27] These assignments were based on ^{29}Si NMR spectroscopy of the mixture of Me_3SiOEt/ethanol (containing 10 vol% of [D_6]ethanol)/THF/H_2O/HCl = 1:3:2.2:1:0.001 after 1.5 h of reaction (data not shown). Three signals appeared at 16.1, 13.0, and 7.2 ppm, which were unambiguously assigned to Me_3SiOEt, Me_3SiOH, and $Me_3Si{-}O{-}SiMe_3$, respectively.
[28] Hybrid xerogels were prepared from the DMDES–BTESM, MTES–BTESM, and TEOS–BTESM mixtures with molar ratios DMDES/BTESM/ethanol/H_2O/HCl = 6:3:36:30:0.06, MTES/BTESM/ethanol/H_2O/HCl = 6:3:36:36:0.06, and TEOS/BTESM/ethanol/H_2O/HCl = 6:3:36:42:0.06, respectively.
[29] T. Asefa, M. J. MacLachlan, H. Grondey, N. Coombs, G. A. Ozin, *Angew. Chem.* **2000**, *112*, 1878–1881; *Angew. Chem. Int. Ed.* **2000**, *39*, 1808–1811.
[30] W.-H. Zhang, B. Daly, J. O'Callaghan, L. Zhang, J.-L. Shi, C. Li, M. A. Morris, J. D. Holmes, *Chem. Mater.* **2005**, *17*, 6407–6415.
[31] L. Zhang, H. C. L. Abbenhuis, Q. Yang, Y.-M. Wang, P. C. M. M. Magusin, B. Mezari, R. A. Santen, C. Li, *Angew. Chem.* **2007**, *119*, 5091–5094; *Angew. Chem. Int. Ed.* **2007**, *46*, 5003–5006.
[32] K. Landskron, G. A. Ozin, *Science* **2004**, *306*, 1529–1532.
[33] H. W. Hillhouse, J. W. van Egmond, M. Tsapatsis, J. C. Hanson, J. Z. Larese, *Microporous Mesoporous Mater.* **2001**, *44–45*, 639–643.
[34] G. J. A. A. Soler-Illia, E. L. Crepaldi, D. Grosso, C. Sanchez, *Curr. Opin. Colloid Interface Sci.* **2003**, *8*, 109–126.
[35] G. J. A. A. Soler-Illia, P. Innocenzi, *Chem. Eur. J.* **2006**, *12*, 4478–4494.
[36] S. Yang, P. A. Mirau, C.-S. Pai, O. Nalamasu, E. Reichmanis, E. K. Lin, H.-J. Lee, D. W. Gidley, J. Sun, *Chem. Mater.* **2001**, *13*, 2762–2764.
[37] F. K. de Theije, A. R. Balkenende, M. A. Verheijen, M. R. Baklanov, K. P. Mogilnikov, Y. Furukawa, *J. Phys. Chem. B* **2003**, *107*, 4280–4289.
[38] B. D. Hatton, K. Landskron, W. Whitnall, D. D. Perovic, G. A. Ozin, *Adv. Funct. Mater.* **2005**, *15*, 823–829.

Received: August 9, 2007
Revised: October 29, 2007
Published online: February 1, 2008

